

The Egyptian International Journal of Engineering Sciences and Technology

https://eijest.journals.ekb.eg/

Vol. 52 (2025) 55-68

DOI: 10.21608/eijest.2025.349906.1317



Structural Performance of Perforated Steel Beam Columns" A Parametric Study

Mona M. Fawzy*

Civil Engineering Program, The Higher Institute of Engineering, El-Shorouk Academy, Dahyet Al-Nakhil, Cairo, 11837, Egypt

ARTICLE INFO

ABSTRACT

Article history:

Received 12 January 2025 Received in revised form 12 March 2025 Accepted 12 March 2025 Available online 12 March 2025

Keywords:

Beam columns Analytical study Flexural buckling Web opening Stiffener The objective of this research is to conduct a parametric study for unstiffened and stiffened steel beam columns with openings and develop their design equations. Since the presence of openings in the beam columns is inevitable, maintaining strength is crucial. Steel beam columns with openings are stiffened with two different stiffening schemes around the opening: horizontally and vertically. Unfortunately, there are no available design equations for steel beam columns with openings except Darwin's' which are suitable for compact beams' web. The parameters studied are the opening shape, web slenderness (non-compact and slender), the effect of stiffening, and opening location with respect to the support. Interaction curves are plotted according to analytical finite element models. Both lateral-torsional buckling and local buckling are observed. Using a square opening instead of a rectangular opening result in a rise in the moment's capacity of up to 18%. Moment resistance can be increased by up to 19% and 20%, respectively, when beam columns are stiffened with vertical and horizontal stiffeners around the opening. The normal and moment resistances decreased by up to 2% and 10%, respectively, when the opening was moved from support to near mid-span. Finally, the proposed design equations for beam columns with openings give agreeable results in the moment and normal strengths.

1. Introduction

Web holes are frequently included in structural parts to accommodate ventilation ducts and service passageways. Despite using circular openings more frequently in commercial buildings, there are situations when using square or even rectangular web holes rather than circular ones is necessary. Currently, there is a trend toward using openings that are getting broader and wider. Without any doubt, the load-carrying capacities of steel beam-columns are severely penalized by the existence of web holes. The

relevant literature is reviewed, and then analytical work is discussed to produce a thorough parametric analysis of the load-carrying capacities of stiffened steel beam-columns with different web opening shapes and sizes and prepare design equations.

2. Background

Studies on cold-formed, thin-walled steel columns with an opening have been studied experimentally by Sadjad and Al-Thairy [1] and Magdi et al. [2]. Different parameters are considered such as opening

^{*} Corresponding author. Tel.: 20122451411 E-mail address: m.fawzy@sha.edu.eg

shape, location, and web slenderness. Their studies show that the behavior of web panels in steel members under compression is characterized by buckling. Therefore, their resistance is governed by local or global buckling or yielding, depending on their slenderness. The risk of instability is reduced when stiffeners are used, which was not included in research. Both experimental and analytical studies are conducted by Bougoffa et al. [3] on compressed stiffeners where either plasticization or local stiffener buckling occurs. EL-Ghazaly and A. N. Sherbourne [4] studied the effect of stiffener size on column web buckling. Both Xu et al. [5] and Bougoffa et al. [6] studied experimentally and analytically different transverse stiffeners including single-sided, doublesided and partial stiffeners. Perforated steel beams were also studied by taking into consideration the effect of web opening shape and load configuration. Nawar et al. [7] investigated the minimum span-todepth ratio of the beam. Nawar et al. [8] continued their studies on solid web I-shaped under blast loading. Although, many researchers studied beam columns either hollow or filled with concrete, nevertheless, AISC, [9] and [10] don't include design equations that can be used for steel beam columns with openings. The closed guide for designing steel and composite beams with web holes was prepared by Darwin [11] and [12] under the supervision of the American Institute of Steel Construction's research committee as shown in (1). Moment shear interaction is suggested using the ratio between factored load at an opening and design strength. This can only be used in compact beams where there is a shortage in the guidelines of beam columns with openings. Darwin [11] guidelines provide interaction equations for moment-shear interaction for both unstiffened and stiffened beams in (1), (2), and (3).

$$\left(\frac{M_u}{\phi M_m}\right)^3 + \left(\frac{V_u}{\phi V_m}\right)^3 \le R^3, R = 1 \tag{1}$$

Where

 Φ is the resistance factor, it is equal to 0.9 for bending and shear

 $M_{\rm m}$ is the nominal capacity of steel member with web opening under pure bending

 M_p is the capacity of steel member without web opening = $F_\nu Z$

M_u is the actual bending moment

V_u is the actual shear force

$$V_p = \frac{F_y dt_w}{\sqrt{3}}$$

$$V_{mb} = V_{nb} \alpha_{vb}$$

$$\begin{array}{l} \mathbf{V_{mt}} = \mathbf{V_{pt}} \boldsymbol{\alpha_{vt}} \\ \boldsymbol{\upsilon} = \frac{a_0}{s_b} \text{ and } \boldsymbol{\mu} = \frac{p_r \, d_r}{v_{pb} s_b} \\ \boldsymbol{\upsilon} = \frac{a_0}{s_t} \text{ and } \boldsymbol{\mu} = \frac{p_{rd_r}}{v_{pt} s_t} \end{array}$$

R is the ratio of moment or shear to design capacity at opening

For unstiffened members

$$M_m = M_p \left[1 - \frac{\Delta A_s \left(\frac{h_0}{4} + \epsilon \right)}{z} \right] \tag{2}$$

$$\Delta A_s = h_0 t_w$$

$$\alpha_v = \frac{\sqrt{6 + \mu}}{v + \sqrt{3}} \le 1$$

$$v = \frac{a_0}{s_b} \text{ and } \mu = \text{zero for top tee}$$

$$v = \frac{a_0}{s_t} \text{ and } \mu = \text{zero for bottom tee}$$

h₀ is the depth of opening

tw is the thickness of web

e is the eccentricity of opening

Z is the plastic section modulus of member without opening

For stiffened members

$$M_m = M_p \left[1 - \frac{t_w \left(\frac{(h_0)^2}{4} + h_0 \varepsilon - \varepsilon^2 \right) - A_r h_0}{z} \right] \le M_p (3)$$

$$\Delta A_s = h_0 t_w - 2 A_r$$

$$A_r = b_{st} t_{st}$$

$$P_r = F_y A_r \le \frac{F_{ytw} a_0}{2\sqrt{3}}$$

F_v is the yield strength of steel

 d_r is the distance from the outside edge of the flange to the centroid of the reinforcement

S_bis depth of bottom tee as shown in Fig. 1

S_t is depth of top tee as shown in Fig. 1

Fig. 1. Upper and lower tees for unstiffened and stiffened sections with openings

However, there are limits to applying these guidelines, for instance, compact beams only. Although it is only applicable to compact sections, this design guide offers a uniform method for designing structural steel members with reinforced or unreinforced web holes. Additionally, the majority of codes and studies focused on perforated beams with compact sections. To keep construction costs as low as possible, the majority of steel beams are

manufactured as non-compact or slender sections. This highlights the need to research these kinds of web-opening steel beams to determine their strength in the presence or absence of reinforcement. Fattouh and Shahat [13] and [14] studied his guidelines on non-compact and slender beams. Their conclusions show that Darwin's [9] guidelines can be used when the opening is located at high shear or moment zone locations. On the contrary, these guidelines are not suitable for zones with combined shear and moment, especially with rectangular openings.

Magdi et al. [14] proposed modifying Darwin's [11] guidelines to study steel beam-columns with openings under the influence of various parameters by adding a term for normal force to the equation as shown in equation (4). The study included the effect of opening shape and location from support only with a limited number of analytical finite element model results. Thus, further research is required to incorporate the effects of different stiffening schemes around the opening of steel beam-columns among the other parameters and at the same time expand the number of analytical finite element results studied. Hence, this research studied the influence of opening shape, location from support, web slenderness, and the effect of stiffening the web around the opening horizontally and vertically.

$$\left(\frac{M_u}{\phi M_m}\right)^3 + \left(\frac{N_u}{\phi N_m}\right)^3 + \left(\frac{v_u}{\phi V_m}\right)^3 \le R^3, \ R = 1 \tag{4}$$

Where

$$\begin{split} N_{m} &= N_{mb} + N_{mt} \leq N_{p} \\ N_{p} &= F_{cr} A_{g} \\ N_{mb} &= F_{cr} A_{b} \\ N_{mt} &= F_{cr} A_{t} \\ F_{cr} &= \frac{0.877 \ F_{y}}{(A_{c})^{2}} \text{For } A_{c} > 1.5 \\ F_{cr} &= 0.658^{\lambda_{c}^{2}} F_{y} \text{ For } A_{c} \leq 1.5 \\ A_{c} &= \frac{KL}{\pi r} \sqrt{\frac{F_{y}}{E}} \end{split}$$

 A_g is the gross area of the section A_t is the area of the top tee A_b is the area of the bottom tee F_{cr} is critical buckling strength A_c is the slenderness parameter of the beam-column R is the radius of gyration about the axis of buckling E is the modulus of elasticity K is an effective buckling length factor

3. Finite element model

Nonlinear static analysis is conducted using the ANSYS software [15] where shell element SHELL181 is used similar to the finite element model

prepared by Magdi et al., [2]. The finite element model is meshed into elements with an aspect ratio equal to 1. Shell element SHELL181 consists of four nodes, each having six degrees of freedom: x, y, and z translations as well as rotations around the x, y, and z axes. The element only has translational degrees of freedom if the membrane option is selected. When creating meshes, the degenerate triangular option should only be utilized as filler pieces. Both nonlinearities in the material and geometry are studied where the bilinear model of steel material with a yield stress of 240 MPa is as shown in Fig. 2. The tangential modulus of elasticity is taken equal to 0.01 of modulus of elasticity. The model nodes were merged at the location between the flange and web and between the stiffener and other model parts.

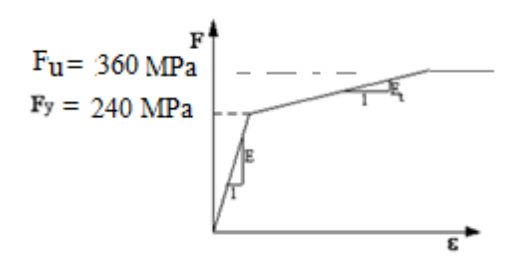


Fig. 2. Bilinear stress-strain curve of material in the analytical finite element model of the author compared to the experimental work of Magdi et al., [2]

4. Finite element model verification

A comparison is made between the experimental work of Magdi et al., [2] and the author's finite element model that is explained in the previous section. Magdi et al. [2] investigated the effects of web openings on the capacity of steel beam-columns. Twelve simply supported 2400 mm-long I sections are tested with flange dimensions 100*5 mm, and web 320*5 mm. Specimens are incrementally loaded till failure in the vertical direction. The vertically concentrated load at the mid-span with horizontal load is applied constantly, which is equal to the plastic capacity of specimens without opening as defined in the background section. No stiffeners are used at loading positions, they are only found at support with dimensions 300*5 mm. A tensile test is conducted on specimens according to DIN 50125 [16] indicates that steel yield strength is 245 MPa and the ultimate strength is 387 MPa for specimens. The modulus of elasticity of steel E is 2.047*105 MPa. All openings are at mid-span with different sizes and shapes of the openings are found in Table (1). The comparison between Magdi et al., [2] and the author's finite element models show good agreement of results with an average of 6% and a standard deviation of 8%.

Web buckling at the compression zone in the compression flange of specimens is shown in Figs. from 3 to 5 of specimens COA, C4, and C8. Fig. 6 shows the load-deflection curve of different specimens compared to the proposed finite element model proposed by the author. The comparison between experimental and finite element load and displacement of specimen COA shows differences equal to 7% and 1% respectively. Specimen C4 shows that the load and displacement of finite element exceeds experimental results by 9% and 10% respectively. Finally, specimen C8 shows 10% variation in both load and displacement when comparing between finite element and experimental results, hence, the results match each other well.

Table (1) Dimensions of experimental work of Magdi et al., [2]

				F.1. 1. 1(1N)						
				Failure load (kN)						
Specimen	Shape of opening	Opening dimension (mm)	Failure mode	EXP by Magdi et al., [2]	ANSYS by author	%Difference				
C0A	NO	-		97	108	11				
C1	Square	160*160		71	77	8.4				
C2	Rectangular	320*160		64	70	9.3				
C3	Circular	160		74	83	12				
C0B	NO	-	gui	66	76	15				
C4	Square	160*160	Local Buckling	52	56	7.7				
C5	Rectangular	320*160	al B	49	49	-				
C6	Circular	160	Loc	55	49	10.9				
C0C	NO	-		48	55	14.6				
C7	Square	160*160		38	42	10.5				
C8	Rectangular	320*160		32	35	9.3				
C9	Circular	160		46	41	10.9				
					Av.	9.96				
					St. dev.	2.2				

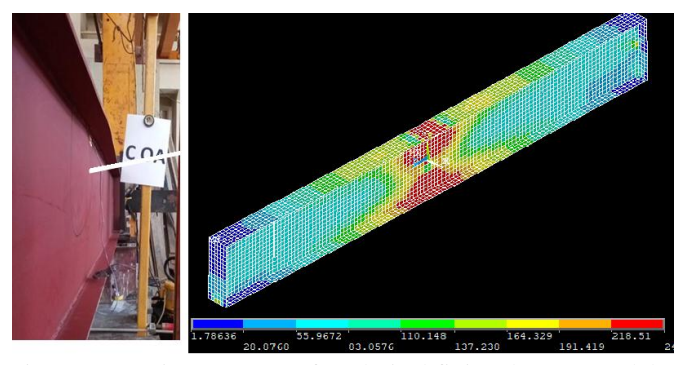


Fig. 3. Von Mises stresses of analytical finite element model by the author to verify experimental work of specimen C0A prepared by Magdi et al., [2]

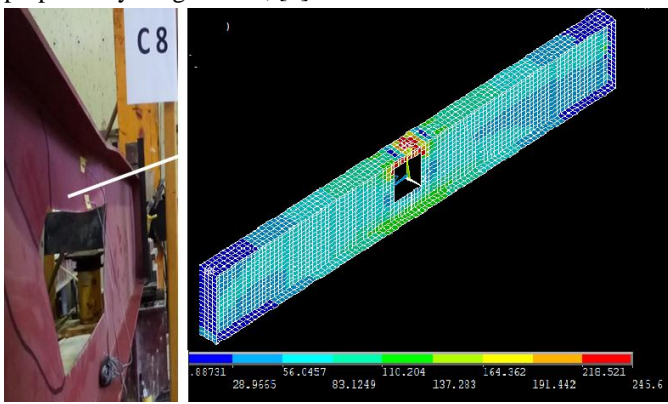


Fig. 4. Von Mises stresses of analytical finite element model by author to verify experimental work of specimen C4 prepared by Magdi et al., [2]

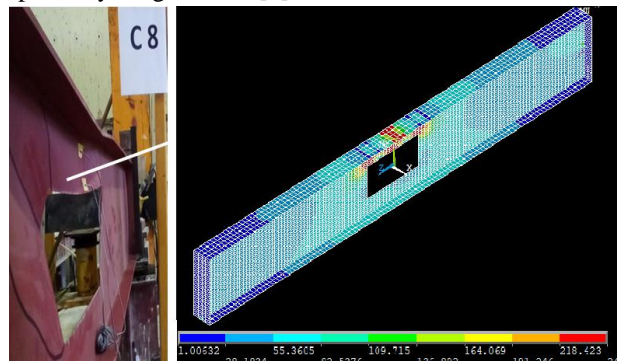


Fig. 5. Von Mises stresses of analytical finite element model by author to verify experimental work of specimen C8 prepared by Magdi et al., [2]

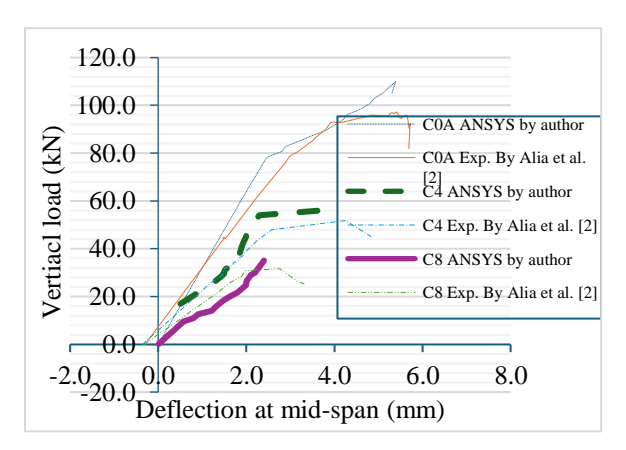


Fig. 6. Deflection at mid-span versus vertical load

Another verification is conducted between the author's finite element model and experimental research by Sadjad and Al Thairy [1]. Researchers investigated the effects of web opening on the axial load capacity of thin-walled, cold-formed steel columns 100*100*2 through experimental studies. Seven 500 mm-long small-scale cold-formed box sections CP, C1, C2, C3, C4, C5, and C6 are tested. specimens' dimensions and geometrical properties are determined in Fig. 7. The specimens are loaded with compression force equal to the maximum capacity of the specimen. The LVDTS placed at the top and mid-span of the specimens are used to measure the axial and lateral displacements, respectively. Specimens are subjected to axial compressive load increments till failure. A bilinear model with yielding is based on a 201x103 MPa Young's modulus. 534 MPa is the maximal strength, and the yield is equal to 420 MPa. Good agreement in results is observed in Table (2) where the average is 9% and the standard deviation is 6%.

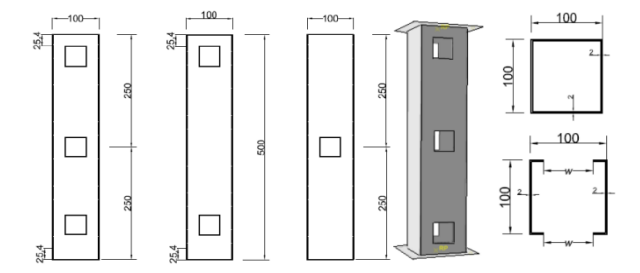


Fig. 7. Experimental work dimensions of Sadjad and Thairy [1].

Table (2) Comparison between the experimental work of Sadjad and Al Thairy [1] and the author's finite element model

Specime ns	Opening shape	Opening dimensio	width (w/W)	Number of web	Failure	Exp. (kN)	Author (kN)	% Differen ce
СР	Reference	N/A	N/A	N/ A		212	201	5.2
C1	Square	44.3x44. 3	0.443	1		171	197	15.2
C2	Square	44.3x44. 3	0.443	2		170	192	13
C3	Square	44.3x44. 3	0.443	3		150	163	8.6
C4	Rectangular	65x30.2	0.650	1		165	184	11.5
C5	Rectangular	65x30.2	0.650	2		163	179	9.8
C6	Rectangular	65x30.2	0.650	3		160	178	11.2
							Av. St.	10.6
							dev	2.97

5. Parametric study

The studied finite element model is 2500 mm long with two 150 x 6 mm flange plates and a 340 mm high web plate with web thicknesses equal to 2 mm and 3 mm. Stiffeners are added at loading positions with thicknesses are 16 mm with a length of 328 mm in the web direction and 150 mm in the flange direction. These dimensions are used in the finite element models to create non-compact and slender built-up sections with compact stiffeners that satisfy the needs of both commonly used and economical sections. Axial load is applied at beam-column with vertical loads at third and two-thirds spans where stiffeners are applied at loading positions. To simulate hinged support, displacements in three directions are prevented at one end of the beam column. The roller support at the other end of the model is where

displacements in the Y and Z axes are prevented as shown in Fig .8 where stiffeners are also used at those positions. The results are plotted in interaction curves where each curve is the result of five loading cases: normal capacity of the section without opening (N) only, bending capacity of the section without opening (M) only, 0.5N and M, 0.75N with 0.25M, and 0.5M and N.

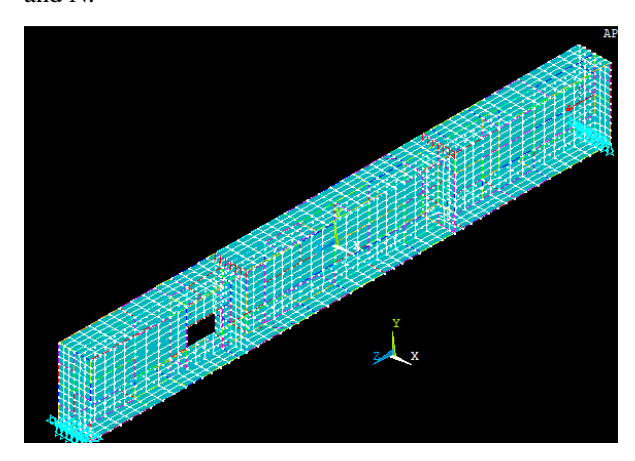


Fig. 8. Loading and end conditions of all finite element models

The parametric variables of the studied beamcolumn are shown in Fig. 9. The first factor is the opening shape square or rectangle, h₀ is the dimension of the opening in the vertical direction and a₀ is the dimension of the opening in the horizontal direction. The opening shape is square when both a₀ and h₀ are equal whereas the opening shape is rectangular otherwise. The first factor studied is the ratio of the opening height (h₀) to the depth of the beam column (d), where (h_0/d) equals 0.5 and 0.7, these ratios are used in common practice. The second factor is web slenderness where the studied web thicknesses of 2 mm and 3 mm, the third factor is the stiffening technique, where both longitudinal (S-S1) and transverse stiffeners (S-S2) are studied. The fourth factor is the opening position, where (D/L%) = 15%, 25%, and 40% is the ratio of the distance from support to the centerline of opening (D) to beamcolumn span (L) as shown in Fig. 9. Square openings with dimensions of 170 mm and 170 mm and a ratio of a₀/h₀ equal to 1 are selected. The studied dimensions of rectangular openings are 121.42 mm and 238 mm. These measurements were chosen to have the same opening area in all square and rectangular models which helps study the effect of opening shape on the results. The dimensions of one side longitudinal stiffeners (S-S1) that are used around the openings are 1.5 in length, widths like flange width, and 16 mm thickness. As for one-side transverse stiffeners (S-S2), their lengths are equal to the web depth with a width equal to the flange width

and 16 mm thickness, so all stiffeners are class 1 according to AISC [9] as shown in Fig. 9. Both letters and numbers are utilized in identifying specimens for example, IN-US-0.5-15% means non-compact unstiffened (US) I-shaped beam column with $h_0/d=0.5$ and D/L=15%. Another example is IS-S-S1-0.7-40% which stands for slender stiffened with longitudinal stiffener (S-S1) I shaped beam column with $h_0/d=0.7$ and D/L=40%.

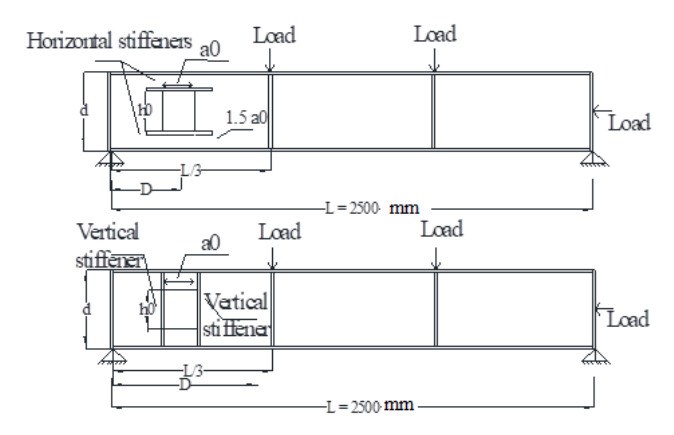


Fig. 9. Configuration of beam-column studied in parametric study

6. Parametric Study Results and Discussions

The results of finite elements are displayed as interaction diagrams for steel beam-columns under axial loads at the end support and concentrated loads at one-third and two-thirds of the beam-column span in the vertical direction. In the interaction curves, to normalize the results, analytical finite element model results of perforated sections are divided by results of analytical finite element model results without opening.

6.1. Failure criteria and modes

Buckling modes varied depend upon loading condition, opening position (D/L), and presence of stiffener as shown in Figs. 10 and 11. When the beam column is loaded axially local buckling occurs as shown in Fig. 10. Meanwhile, when the model is subjected to combined moment and normal, both lateral and local buckling occurs as shown in Fig. 11. Additionally, Vierendeel bending moment is observed as a result of shear transfer in the opening vicinity as shown in Fig. 12. This Vierendeel failure mechanism is especially noticed as the opening dimensions increases and the opening is located in the critical shear zone.

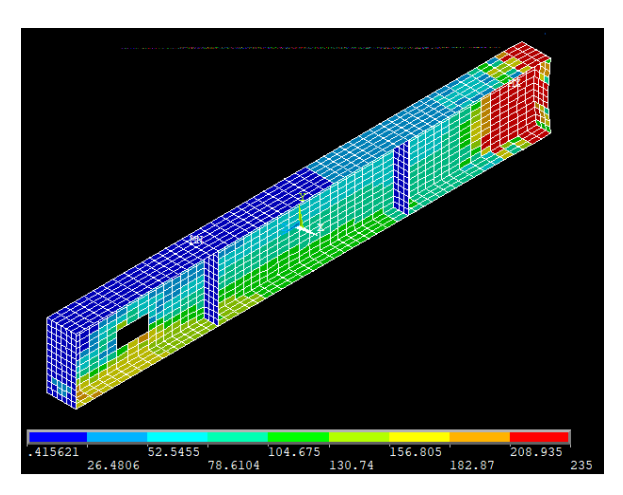


Fig. 10. Local buckling of beam-column under axial loading with D/L 15%

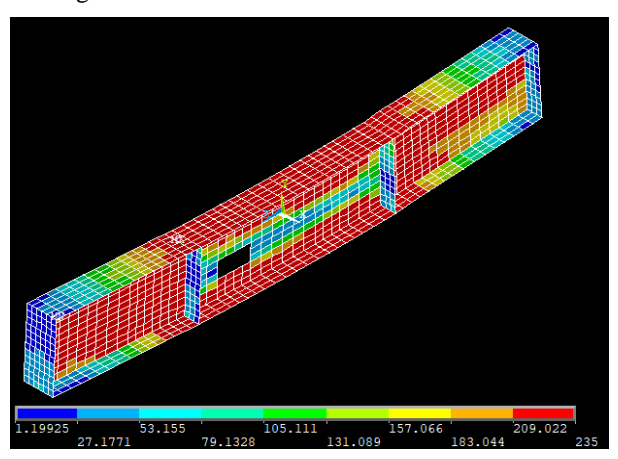


Fig. 11. Lateral torsional and local buckling of beam-column loaded under axial and moment with D/L 40%

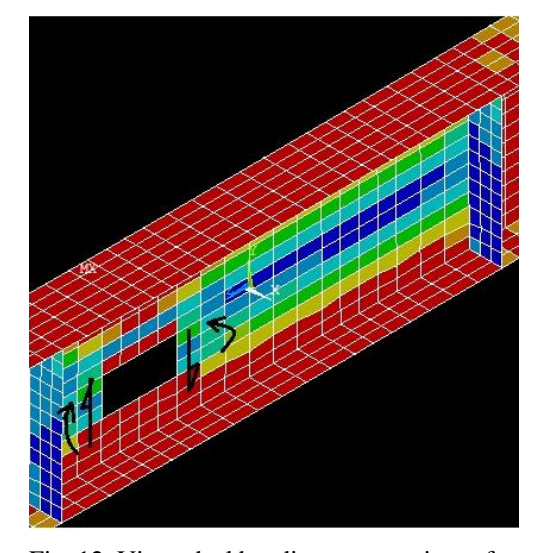


Fig. 12. Vierendeel bending moment in perforated beam-column

6.2. Effect of web opening shape

Analytical finite element models are used to prepare interaction diagrams. Square opening $(h_0/d=0.5)$ and rectangular web opening $(h_0/d=0.7)$ interaction diagrams are shown in Figs. 13 to 15. Uniform stress distribution occurs around square openings more than rectangular ones. For US noncompact sections, when using a square opening instead of a rectangular opening the ratio of M/M_n rises by up to 12% with D/L equals 40% with a corresponding increase in N/N_n by up to 13%. Regarding S-S1 sections, the rise in the ratio of M/M_n is up to 18% with D/L equals 15% without a change in the ratio of N/N_n when using a square opening instead of a rectangular one. As for S-S2 sections, the ratio of M/M_n increases by up to 16% with a constant N/N_n ratio with D/L equals 40%. For slender sections with D/L equals 25%, the ratios of M/M_n are enhanced by up to 10% with the same ratios of N/N_n when a square opening is used instead of a rectangular one. Overall, no significant surpassing is noticed in slender sections because of the loss in the overall capacity of the sections.

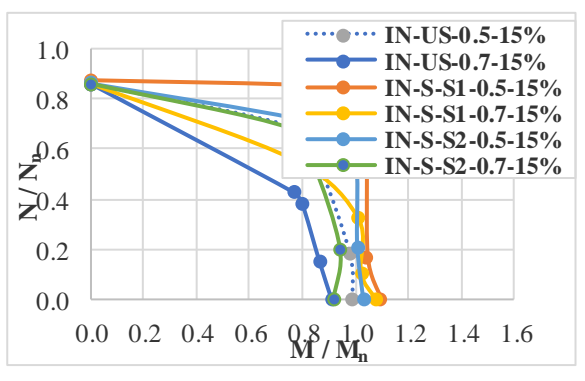


Fig. 13. Influence of web opening shape for non-compact specimens where D/L% equals 15%

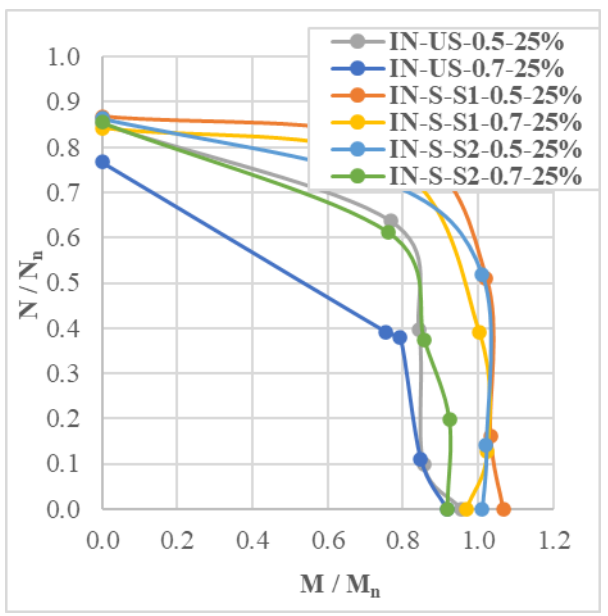


Fig. 14. Influence of web opening shape for non-compact specimens where D/L% equals 25%

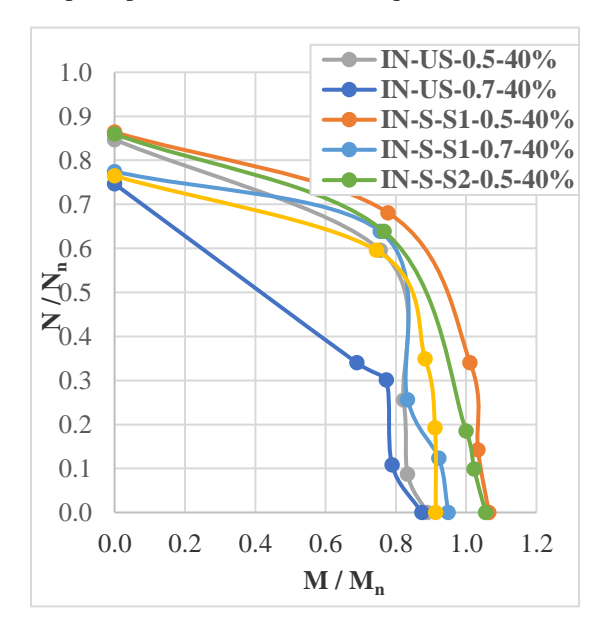


Fig. 15. Influence of web opening shape for non-compact specimens where D/L% equals 40%

6.3 Effect of web slenderness

Since web plate height is constant throughout the study, studying web thickness equal to 2 mm represents a slender web. On the other hand, studying web thickness equal to 3 mm represents a noncompact web. The effect of replacing a slender web with a non-compact one is studied in this section. The first results of beam-columns with square openings (h₀/d=0.5) are shown in Figs. From 16 to 18. For

sections with D/L equals 15% and 25%, the ratio of M/M_n displays an escalation by up to 11% in the US sections. Meanwhile, the ratio of N/N_n is enlarged by 26% in all sections but for D/L equals 40%, the ratio of M/M_n increases by up to 17% in the S-S2 sections. Meanwhile, the ratio of N/N_n is magnified by up to 27%, in all sections which emphasizes the role of the web when the beam-column is under the effect of the normal force. Second when sections with rectangular openings (h₀/d=0.7) are studied as shown in Figs. From 19 to 21, sections with D/L equal to 15% and 25% show a higher ratio of M/M_n by up to 8% in both US and S-S1 sections. A rise in the ratio of N/N_n by about 26% is perceived in all sections at D/L equals 15%. When D/L equals 40%, there is no improvement in the ratio of M/M_n for all US, S-S1, and S-S2 sections respectively. The enhancement in the ratio of N/N_n is equal to 11%, 14%, and 13% in the US, S-S1. and S-S2 sections respectively. It is concluded that the slender web is fragile under the effect of normal force especially in the presence of rectangular openings because of the non-uniform stress distribution around the opening in the presence of a weak web.

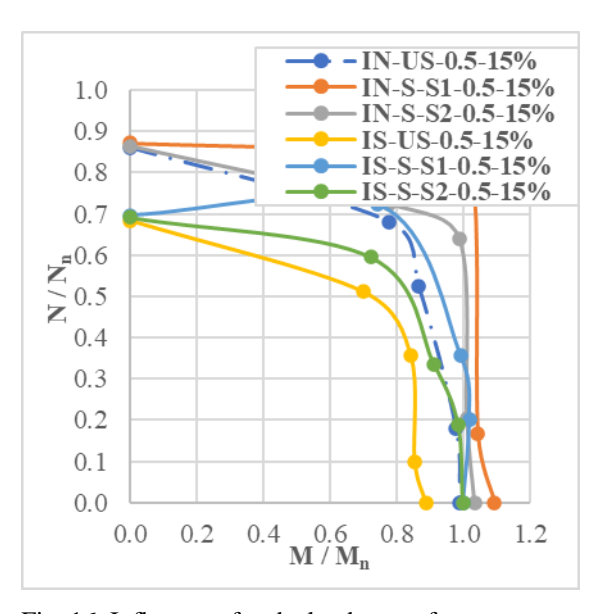


Fig. 16. Influence of web slenderness for non-compact and slender specimens where D/L% equals 15% with $h_0/d=0.5$

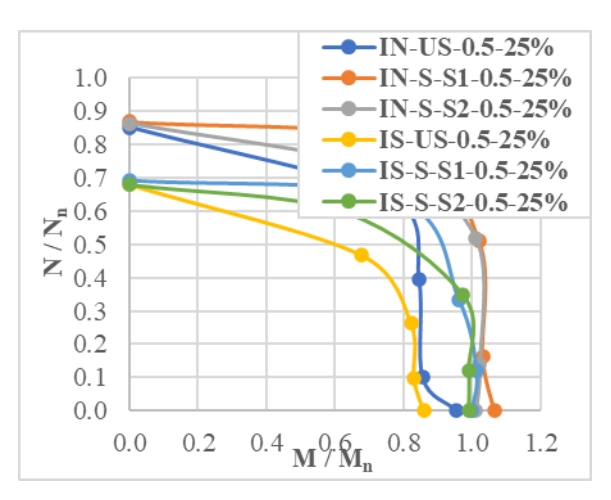


Fig. 17. Influence of web slenderness for non-compact and slender specimens where D/L% equals 25% with h_0/d =0.5

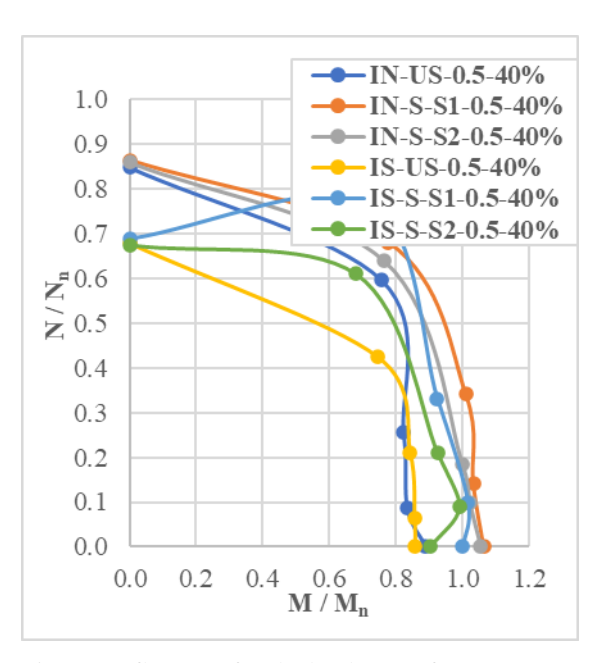


Fig. 18. Influence of web slenderness for non-compact and slender specimens where D/L% equals 40% with $h_0/d=0.5$

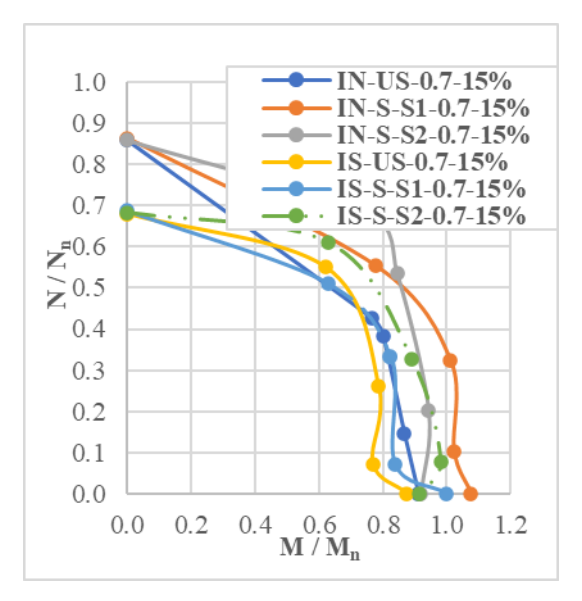


Fig. 19. Influence of web slenderness for non-compact and slender specimens where D/L% equals 15% with $h_0/d=0.7$

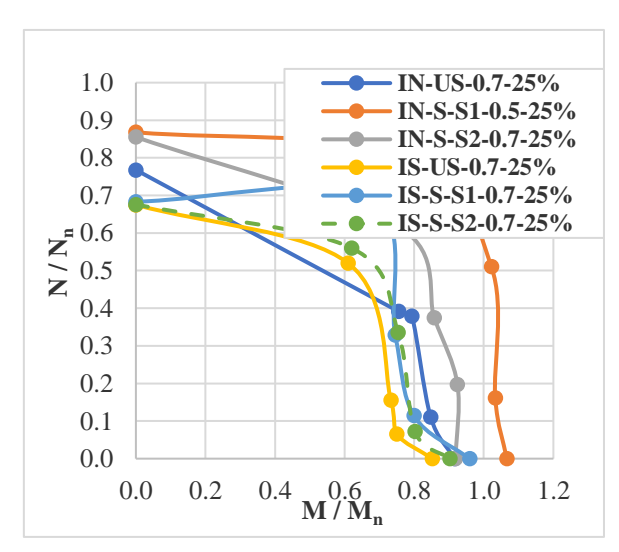


Fig. 20. Influence of web slenderness for non-compact and slender specimens where D/L% equals 25% with $h_0/d=0.7$

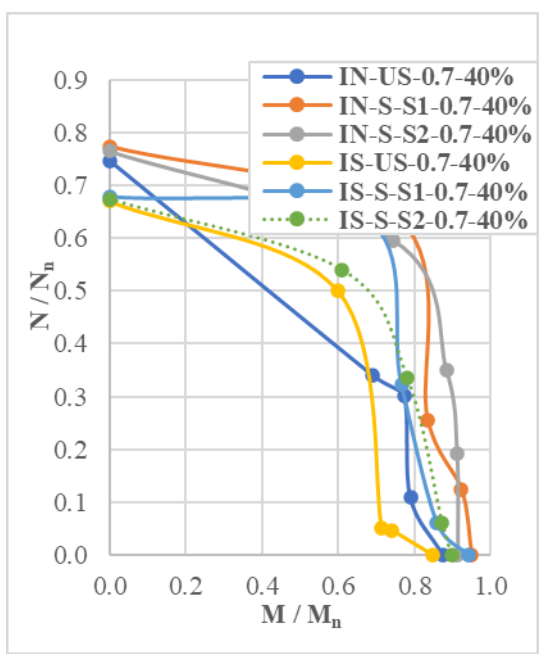


Fig. 21. Effect Influence of web slenderness for non-compact and slender specimens where D/L% equals 40% with $h_0/d=0.7$

6.4 Effect of stiffening

Two stiffening schemes around the opening are studied in this research paper, the first one uses longitudinal (horizontal stiffener, S-S1), while the other stiffening scheme uses transverse stiffeners (vertical stiffener, S-S2) as shown in Fig. 9. The dimensions of the used stiffeners are mentioned in the parametric study section. To highlight the effect of stiffeners, S-S1 and S-S2 sections are compared to US sections.

First, for non-compact sections $h_0/d=0.5$ and D/L equals 15% and 25% as shown in Figs. 16 and 17 respectively. Models with longitudinal stiffeners (S-S1) escalate the ratio of M/M_n by up to 11% with an almost constant ratio of N/N_n when compared to similar US sections because forces are transmitted around the opening in the presence of the stiffener; besides the web plays the main role in moment resistance while normal stresses are distributed equally all over the section. When stiffening the section with transverse stiffeners i.e. S-S2 section a rise of 4% in the ratio of M/M_n with no change in the ratio of N/N_n. Furthermore, non-compact sections with h₀/d=0.5 and D/L equals 40%; the enhancement is 20% and 19% in the ratio of M/M_n with constant ratio of N/N_n respectively in S-S1 and S-S2 sections as shown in Fig. 18. Sections with $h_0/d=0.7$ and D/L equals 15%, 25%, and 40% record same ratio of N/N_n in case of stiffening US sections with S-S1 and S-S2 sections. On the contrary, at D/L equals 15% when the S-S1 and S-S2 sections are compared to the US sections the ratio of M/M_n shows 18% and 9% increase respectively as shown in Fig. 19. Other ratios of D/L show lower improvement by up to 9% as a result of comparing S-S1 and S-S2 sections to US sections as shown in Fig. 20. Second, in slender sections with $h_0/d=0.5$ when the ratio of M/M_n in S-S1 is compared to the US section at D/L equals 25% and 40%, the enlargement is up to 16%. Comparing US sections with S-S2 sections, the ratio of M/M_n increases by 12% without any change in the ratio of N/N_n as shown in Fig. 21. Third, in slender sections with $h_0/d=0.7$ when the ratio of M/M_n in S-S1 is compared to the US section at D/L equals 15%, the raise is up to 14% with no obvious change in the ratio N/N_n. Using S-S2 instead of US sections shows a rise in the ratio of M/M_n by 5% with a constant ratio of N/N_n . It is noticed that the ratio N/N_n remains nearly constant in all cases. It can be concluded that using any type of stiffener reduces the effect of web local buckling by transmitting the forces to the vanity around the opening and therefore Vierendeel action decreases.

6.5 Effect of opening location

The main objective of this section is to study the effect of changing the location of the opening in noncompact and slender beam-columns that are either US, S-S1, or S-S2 sections. It is observed that Vierendeel action occurs causing additional moments around the opening. Especially around rectangular openings more than square openings. Since the bending moment increases gradually toward the midspan, then it is established that as the opening approaches the midspan, both stiffness and flexural resistance decrease which complies with Fattouh and Shahat [12]. Therefore, when the opening location is changed from D/L equals 15% to D/L equals 40%, the decrease in both ratio of M/M_n and N/N_n is more than when the opening location is changed from D/L equals 15% to D/L equals 40%. Also, the effect of changing the opening location is more obvious in the US sections than in the S-S1 and S-S2 sections. It is observed that for non-compact US sections with $h_0/d=0.5$, the ratio of M/M_n is lowered by 10% and the ratio of N/N_n is lowered by 2% as shown in Fig. 22 when changing the opening location from D/L equals 15% to D/L equals 40%. While in S-S1 sections with h₀/d=0.5 when the opening is switched from D/L equals 15% to 40%, the decrease in the ratio of M/M_n with constant ratio of N/N_n is 3% as shown in Fig. 23. According to Fig. 24 non-compact S-S2 sections with $h_0/d=0.5$ with different opening locations, 2% loss in the ratio of M/M_n with the same ratio of N/N_n. As can be seen in Fig. 25 non-compact US sections with $h_0/d=0.7$, a reduction by 10%

occurs in both the ratio of M/M_n and N/N_n in both US and S-S1 sections resulting from changing opening location from D/L equals 15% to 25%. On the contrary, the decline in the ratio of M/M_n is 4%, while the ratio of N/N_n is lowered by 13% when D/L changes from 15% to 40% as shown in Fig. 25. and 26. For S-S1 sections, the decline in the ratios of M/M_n and N/N_n is 12% and 10% respectively as shown in Fig. 26. For S-S2 sections, the ratio of M/M_n remains the same when D/L is changed either from 15% to 25% or 40%, while the ratio of N/N_n is decreased by 5% and 11% respectively as shown in Fig. 27. Nearly no change in the ratios of M/M_n and N/N_n is noticed in slender US, S-S1 and S-S2 sections with $h_0/d=0.5$ and 0.7 when D/L changes from 15% to 25% and 40% as can be seen in Fig. 28.

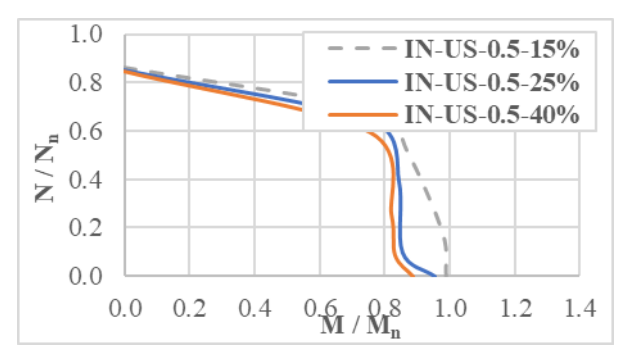


Fig. 22. Effect of changing opening location (D/L equals 15%, 25%, and 40%) for non-compact unstiffened (US) beam columns with h0/d=0.5

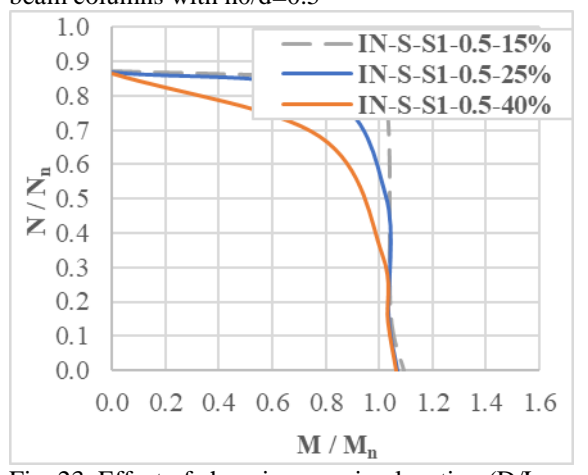


Fig. 23. Effect of changing opening location (D/L equals 15%, 25%, and 40%) for non-compact stiffened beam columns with longitudinal stiffener (S-S1) with $h_0/d=0.5$

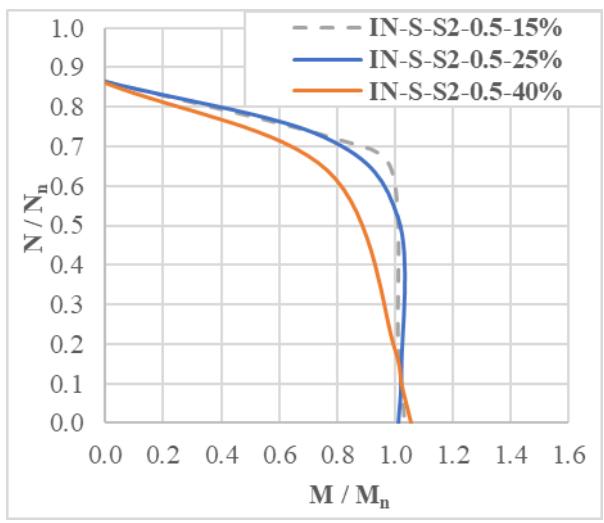


Fig. 24. Effect of chinging opening location (D/L equals 15%, 25%, and 40%) for non-compact stiffened beam columns with transverse stiffener (S-S2) with h₀/d=0.5

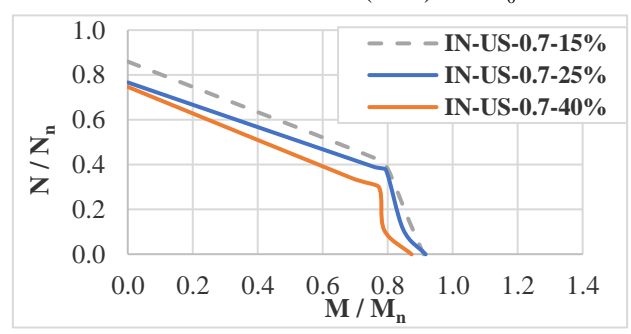


Fig. 25. Effect of chinging opening location (D/L equals 15%, 25%, and 40%) for non-compact unstiffened beam columns (US) with $h_0/d=0.7$

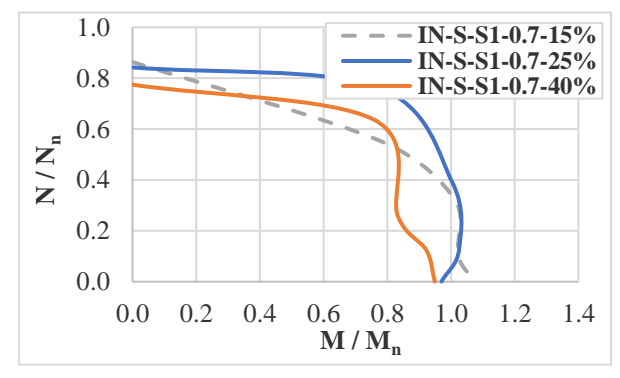


Fig. 26. Effect of changing opening location (D/L equals 15%, 25%, and 40%) for non-compact stiffened beam columns with longitudinal stiffener (S-S1) with $h_0/d=0.7$

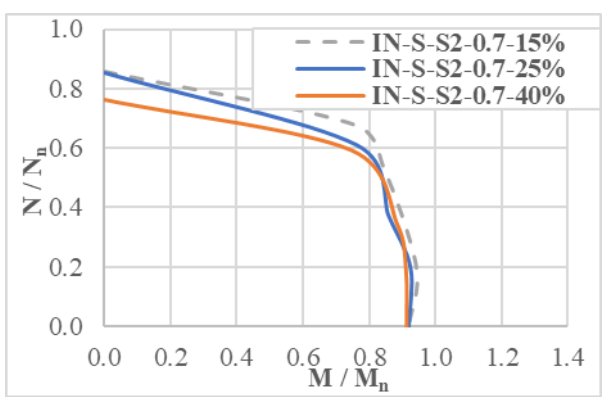


Fig. 27. Effect of chnging opening location (D/L equals 15%, 25%, and 40%) for non-compact stiffened beam columns with transverse stiffener (S-S2) with $h_0/d=0.7$

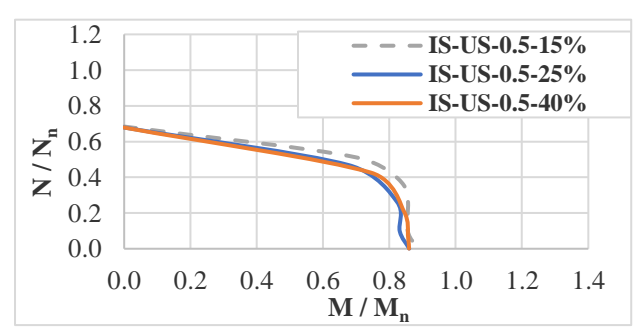


Fig. 28. Effect of chinging opening location (D/L equals 15%, 25%, and 40%) for slender unstiffened (US) beam columns with $h_0/d=0.5$

6.6 Shear force versus changing opening location

Local straining around the opening can be caused by the global shear force acting on the section [7]. Changing the opening location from D/L equals 15% to D/L equals 25% or D/L equals 40% is studied. First, non-compact US, S-S1 and S-S2 sections with $h_0/d=0.5$ when the opening location is moved from D/L equals 15% to 25%, the drop in the reaction at support near the opening is up to 8% meanwhile, when the opening located is changed from D/L equals 15% to 40%, it is lowered by up to 10%. Noncompact US sections with $h_0/d=0.7$ with different opening locations, a reduction by up to 10% occurs in US, S-S1 and S-S2 sections because of changing opening location from D/L equals 15% to 25% or 40%.

7. Perforated Beam-column Design Equation

section presents a comparison between analytical finite element model results (FEM) and proposed EO (4). Finite element model results when compared to proposed EQ (4) results show good agreement in Fig. 29 where FEM exceeds the EQ results by up to 6%. On the other hand, in Fig. 30 FEM results overestimate the normal results by up to 16%. It is noticed that flexural strength is accurately determined regarding the opening location effect. Figs. 31 and 32 show good agreement of FEM results of M/M_P and N/N_P with EO for all values of D/L and h_0/d where the maximum difference is up to 2%. Regarding IN-S-S1 sections, FEM results of M/M_P and N/N_P exceed EQ results for all values of D/L and h₀/d are up to 9% and 16% respectively as shown in Figs. 33 and 34. While FEM results of IS-S-S1 sections of M/M_P and N/N_P are higher than EQ results by up to 0.5% and 2% respectively. It is noticed that moment calculation equations consider the effect of opening shape and location while normal calculation equation considers only the areas of the top and bottom tees.

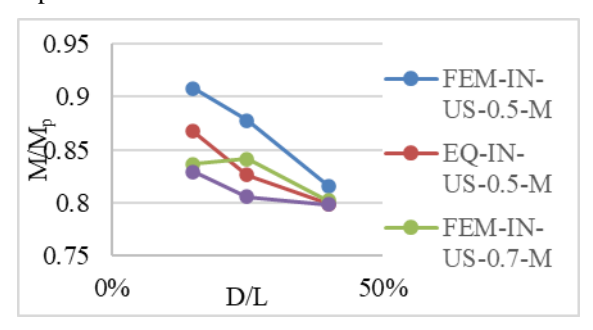


Fig. 29. Moment finite element M/M_P versus equation (4) EQ/ M_P results at D/L equals 15%, 25%, and 40% for unstiffened non-compact beam-columns

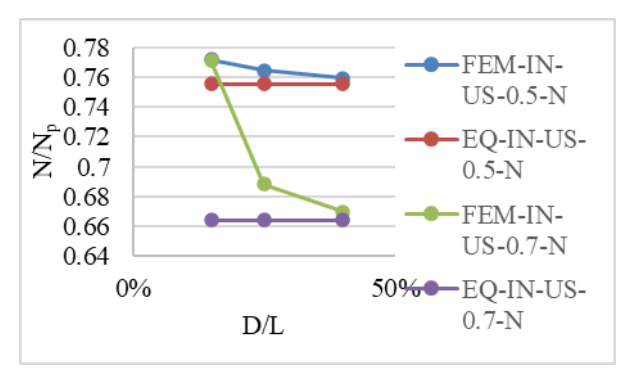


Fig. 30. Normal finite element N/N_P versus equation (4) EQ/ N_P results at D/L equals 15%, 25%, and 40% for unstiffened non-compact beam columns

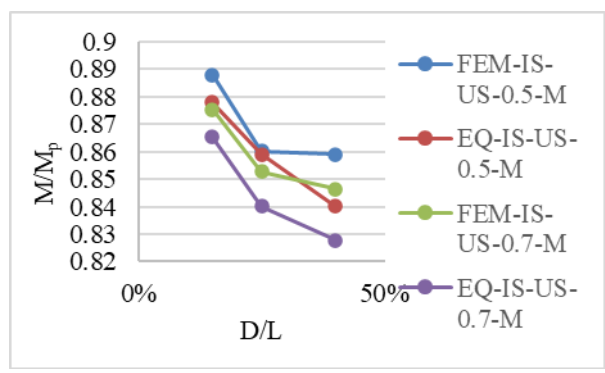


Fig. 31 Moment finite element M/M_P versus equation (4) EQ/M_P results at D/L equals 15%, 25%, and 40% for unstiffened slender beam-columns

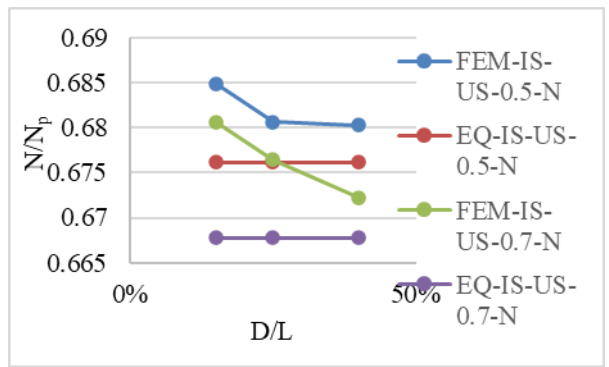


Fig. 32. Normal finite element N/N_P versus equation (4) EQ/ N_P results at D/L equals 15%, 25%, and 40% for unstiffened slender beam columns

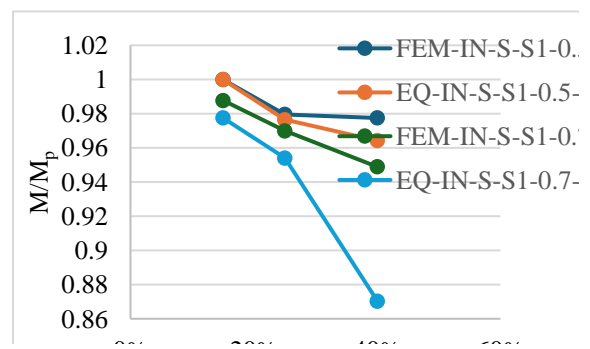


Fig. 33. Moment finite element M/M_P versus equation (4) EQ/ M_P results at D/L equals 15%, 25%, and 40% for stiffened noncompact beam columns

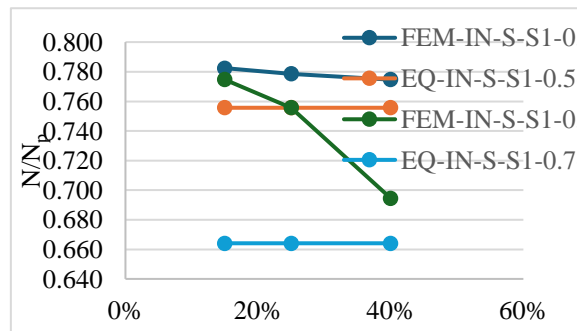


Fig. 34. Normal finite element N/N_P versus equation (4) EQ/ N_P results at D/L equals 15%, 25%, and 40% for stiffened noncompact beam columns

8. Conclusion

This paper discusses the behavior of beam-columns with different variables such as opening shape, web slenderness, stiffening techniques, and opening location are considered. Here are some of the main results:

- When a square opening is used instead of a rectangular one, the moment capacity of non-compact beam-columns is enhanced by 18%, while normal capacity increases by up to 1% especially when using a transverse stiffener. While in slender sections with transverse stiffeners, replacing rectangular opening with square one results in the increase of moment capacity by up to 10% with no significant change in normal capacity.
- Beam columns with longitudinal stiffener show improvement by up to 17% and 27% in both moment and normal capacities respectively when replacing slender web with non-compact web.
- In beam columns with square openings located near midspan, moment resistance is enlarged by 19% when a longitudinal stiffener is utilized and by 20% when a transverse stiffener is used. While normal resistance stays unchanged.
- Stiffening slender beam-columns with either transverse or longitudinal stiffener increases moment resistance by 16% without significant change in normal resistance when the opening is located at midspan.
- Moving the square opening of unstiffened non-compact beam columns from near support to near the middle of the span, moment and normal capacities are lowered by 10% and 2% respectively. While when

- the transversally stiffened rectangular opening is moved towards the middle of the slender beam column, moments decrease by 6% without affecting normal capacities
- The proposed design equation agrees with finite element results at the moment and normal capacities of non-compact and slender beam-columns.

Future work

The author suggests studying stiffened beam-columns with firstly, different loading schemes such as one point load at the middle of the span and distributed load along the span. Secondly, studying different opening shapes such as sinusoidal and hexagonal openings. Thirdly, investigating various materials, incorporating residual stresses, and exploring dynamics.

References

- [1] Al-Jallad A. S., Haitham A.-T.," 2016, Fffect of web opening on the axial load capacity of steel columns with cold formed thin-walled section (CFS) ", Kufa Journal of Engineering, vol.7(3), pp. 13-26.
- [2] Magdi A., Fattouh M. F., Mohammed S., Mona M. F., 2014," Influence of opening location, shape, and size on the behavior of steel beam columns." Steel and composite structures, an int'l journal, vol. 50(1)
- [3] Bougoffa S., Omar M., Sébastien D., Abdelhamid B., Atef D., 2021," Compression zone with partial stiffeners in beamto-column steel connections", Engineering structures, 229.
- [4] Hany E., Archibald S., 1987, Ultimate Strength of Stiffened Symmetrical Welded steel beam-to-column flange connections (1987), Computers and structures, 1986, vol. 16(5), pp. 749-760.
- [5] Xu, Genshu T., Lei Z., 2018," Design of horizontal stiffeners for stiffened steel plate walls in compression", Thin-walled structures, vol.132, pp. 385-397
- [6] Bougoffa S., Omar M., Sebastien D., Abdelhamid B., Atef D., 2022, "Full-length transverse stiffener under compression", The international colloquium on stability and ductility of steel structures.
- [7] Mahmoud N., Ibrahim A., Osama E., Numerical investigation on effective spans ranges of perforated steel beams, Structures, 2020, vol. 25, pp. 398-410.
- [8] Mahmoud N., Ibrahim A., Osama E, Numerical damage evaluation of perforated steel columns subjected to blast loading, Defence Technology,2021.
- [9] AISC 360-10, 2010, Specification for structural steel buildings, American Institute of Steel Construction (AISC), Chicago (IL).
- [10] American institute of steel construction. 2005, Manual of steel construction: Load and resistance factor design specification for structural steel buildings. AISC-LRFD.
- [11] Darwin D. 1990, "Steel and composite beams with web openings - American Institute of Steel Construction" Steel design guide series; No. 2, Chicago, IL.
- [12] Darwin D. and Lucas W.C. 1990, "LRFD for steel and composite beams with web openings." Struct. eng., ASCE; vol. 116(6): pp. 1579- 1593.
- [13] Fattouh M. F. and Mahmoud S., 2015, "Study of Darwin guidelines for non-compact and slender steel girders with

- web openings." IOSR Journal of Mechanical and Civil Engineering (IOSR-JMCE)g, vol. 12(5), pp. 72-85, doi: 10.9790/1684-12517285
- [14] Fattouh M. F. and Mahmoud S., 2015, "Strengthening of web opening in non-compact steel girders." IOSR Journal of Mechanical and Civil Engineering (IOSR-JMCE)g, vol. 12(5), pp. 34-47
- [15] Magdi A., 2023, "The Behavior of steel beam columns with web openings." Ph.D civil engineering, Helwan University.
- [16] ANSYS, 2009, finite element program, Swanson analysis system. Inc., release 12.1.
- [17] DIN 50125,2016, "Testing of metallic materials Tensile test pieces" German Institute for Standardisation (Deutsches Institut für Normung), Berlin, Germany.